Stopping of acoustic waves by sonic polymer-fluid composites

Ph. Lambin and A. Khelif
Département de Physique, Facultés Universitaires N-DP, 61 Rue de Bruxelles, B-5000 Namur, Belgium

J. O. Vasseur, L. Dobrzynski, and B. Djafari-Rouhani
Laboratoire de Dynamique et Structures des Matériaux Moléculaires, UPRESA CNRS 8024, UFR de Physique, Université de Lille 1, F-59655 Villeneuve d'Ascq Cédex, France

(Received 16 January 2001; published 22 May 2001)

A two-dimensional periodic array of air cylinders in water is known to have giant acoustic stop bands [M.S. Kushwaha and B. Djafari-Rouhani, J. Appl. Phys. 84 (1998) 4677]. It is shown in the present paper that hollow cylinders made of an elastically-soft polymer containing air inside and arranged on a square lattice in water can still give rise to large acoustic band gaps. Similar properties can also be obtained with a close-packed array of tubes containing water when arranged on a honeycomb lattice in air. The transmission coefficient of films made of such polymer-fluid composites has been calculated by finite difference time domain method. With film thickness not exceeding 75 mm, a deep sonic attenuation band was found with, in the best cases, a lower limit below 1 kHz and an upper limit above 10 kHz.

DOI: 10.1103/PhysRevE.63.066605 PACS number(s): 43.20.+g, 46.40.−f, 68.60.Bs

I. INTRODUCTION

In a recent publication, Ping Sheng and collaborators reported on the successful realization of a three-dimensional periodic elastic medium presenting band gaps in the domain of acoustic frequencies, while having a period much shorter than the forbidden wavelengths [1]. Such a periodic medium is a sonic crystal, which somehow is an adaptation to elastic waves of the concepts developed earlier for electromagnetic waves in photonic crystals [2]. The design of a composite medium for which the propagation of sound is forbidden in some frequency domains is of great practical interest. Two-dimensional periodic materials are conceptually simpler than three-dimensional sonic crystals and may also present acoustic band gaps [3,4]. It is only recently that this possibility was demonstrated experimentally by several groups [5–8]. On the theoretical point of view, a two-dimensional crystal requires much less computational load than the three-dimensional systems and is therefore more suitable for numerical simulations.

This paper is devoted to the calculation of the transmission coefficient of acoustic waves across a phonic-crystal slab. The technique used is a variant of the finite-difference time-domain (FDTD) method recently developed by several groups in the context of elastic wave propagation [9–12]. As a first example, we consider a square array of polymer tubes with air inside and water outside. The choice of this system, which mixes both fluid and solid media, was dictated by the fact that a periodic array of air cylinders (without a solid envelope) in water is predicted to present giant sonic stop bands [13]. The aim of the present paper is to see to what extent this property is conserved in a realistic situation where the air cylinders are contained in solid tubes immersed in water, and to evaluate the acoustic transmission across a finite thickness of such a medium. This system would have the property of preventing the propagation of sound in a large frequency domain, with the period of the sonic crystal being much smaller than the acoustic wavelength.

If one exchanges the roles of air and water, it appears that water cylinders in air may also present large frequency gaps when arranged on a honeycomb lattice. This system has been considered too, using again polymer tubes to separate the two fluids. Transmission calculations indicate that films of 60–80 mm thickness containing such tubes with air or water either inside or outside can attenuate the sound transmission by two or more orders of magnitude in large intervals of audible frequencies.

II. FORMULATION

We consider a two-dimensional elastic material, possibly a fluid, containing cylindrical or prismatic inclusions parallel to the z direction and having a periodic arrangement in the (x,y) plane. A film of such a composite material is realized by considering a small number of periods in the y direction. The film is bounded by semi-infinite homogeneous media on both sides. The system is infinite in the vertical direction z, and none of its properties depends on z (translational invariance). A traveling wave packet is supposed to arrive from one side and to propagate in the direction of increasing y across the composite-material slab. The wave equation to be solved is

$$\rho(x,y)\,\partial^2\vec{u}/\partial t^2=\vec{\nabla}\cdot\sigma, \tag{1}$$

with ρ the mass density and σ the stress tensor. For simplicity, the displacement field $\vec{u}$ is taken independent on z, and all the materials are supposed to obey the isotropic Hooke's law. In these conditions,

$$\sigma_{xx}=C_{11}\partial u_x/\partial x+C_{12}\partial u_y/\partial y, \tag{2}$$

$$\sigma_{xy}=C_{44}(\partial u_y/\partial x+\partial u_x/\partial y), \tag{3}$$

$$\sigma_{yy}=C_{11}\partial u_y/\partial y+C_{12}\partial u_x/\partial x, \tag{4}$$

with C_{11}, C_{12}, and C_{44} the position-dependent elastic constants. For a given isotropic medium, these constants are not independent. They are related to the longitudinal and transverse speeds of sound c_l and c_t in the usual way: $C_{11} = c_l^2\,\rho$, $C_{44}=c_t^2\rho$, and $C_{12}=C_{11}-2C_{44}$. A fluid is treated as a solid with zero transverse speed of sound.

The second-order time-differential wave equation (Eq. 1) can conveniently be written in a set of canonical, first-order equations:

$$\partial\vec{v}/\partial t=\vec{F}/\rho(x,y), \tag{5}$$

$$\partial\vec{u}/\partial t=\vec{v}, \tag{6}$$

with $\vec{v}$ the velocity field and where $\vec{F}=\vec{\nabla}\cdot\sigma$ is the elastic force per unit volume. These equations are solved by FDTD method, using central differences. The displacement field is calculated at multiple integers of a time step Δt, whereas the velocity is calculated on a time grid shifted by half the step. The solution is subject to the initial conditions

$$\vec{u}(t=0)=g(y)\vec{e}_y, \tag{7}$$

$$\vec{v}(t=\Delta t/2)=-c_l g'(y-c_l\Delta t/2)\vec{e}_y, \tag{8}$$

where $g(y-c_lt)$ is a longitudinal wave packet that at time $t=0$ is localized in the incoming medium and propagates with the velocity c_l of that medium. Here above, g' denotes the derivative of g with respect to its argument. The wave packet is polarized in the y direction and does not depend on x and z. Despite the fact that the initial conditions depend on y only, a two-dimensional solution depending on both x and y is searched for for both u_x and u_y components of the displacement field.

The canonical equations are solved numerically and the time-dependent displacement field is calculated on the other side of the film, in the outgoing medium, where the component $u_y(t)$ is integrated in an interval along the x direction corresponding to a period of the slab. The Fourier transform with respect to time, $U_y(\omega)$, of that quantity is computed. The same algorithm is applied to simulate the propagation of the incoming wave packet $g(y-c_lt)$ in the absence of the film, more precisely when assuming that the incoming medium occupies the whole space. The Fourier transform $G(\omega)$ of that signal is obtained along the same way as here above. The transmission coefficient of the film is then defined as the ratio $T(\omega)=|U_y(\omega)|/|G(\omega)|$. This definition does not ground on energetics consideration and, for that reason, there is no guarantee that $T(\omega)$ will be smaller than one for all frequencies. The definition of T simply assumes that a detector used in an experimental situation will provide a signal proportional to the displacement field $u_y(t)$. In all the calculations we have performed, the x component of the transmitted signal was found to be at least an order of magnitude smaller than $u_y(t)$. The x component of the displacement field was therefore ignored in the definition of the transmission coefficient.

In order to compute the transmission coefficient with a good accuracy, it is important that $G(\omega)$ varies smoothly on a frequency scale ω_0 characteristic of the problem considered. This condition can be realized by taking a wave packet of the form

$$g(y)=A\cos(k_0y)\exp[-(k_0y)^2/2], \tag{9}$$

where $k_0=1.5\omega_0/c_l$. In Fourier space, $G(\omega)$ is the sum of two Gaussians centered at $\omega=\pm k_0c_l$. The mean-square deviation of the two Gaussians is such that all the derivatives of $G(\omega)$ up to order three vanish at the origin. As a result, $G(\omega)$ varies by one percent only in the interval $(0,\omega_0)$.

The wave packet [Eq. (9)] has a spatial extension of the order of half a wavelength, $\lambda_0=2\pi/k_0$, on both sides of its maximum. Therefore, the incident medium in front of the slab needs to have a thickness of the order of λ_0 to contain the initial wave packet. Its maximum at time $t=0$ is placed at the center of this medium slice. On the other side of the slab, the thickness of the outgoing medium is also chosen to be of the order of λ_0 and the transmitted signal $u_y(t)$ is recorded at the end of that slice and integrated along the x interval, as explained above.

The spatial derivatives in the wave equations are also evaluated with a finite difference scheme, using central differences correct to the second order. The x components of $\vec{u}$ and $\vec{v}$ are calculated on the nodes (i,j) of a two dimensional grid with steps Δx, Δy, and the y components are calculated at the center of the meshes [12]. Equations (2)–(4) then require that the components of the stress tensor be evaluated at the centers of the segments joining two neighboring nodes, such as for instance at the coordinates $(i+1/2,j)$. The elastic constants there are defined as the geometric average of the values tabulated on the neighboring nodes, here (i,j) and $(i+1,j)$ [14].

Periodic boundary conditions are applied in the x direction. In the y direction, the so-called Mur conditions [15] are used at the free ends of the incoming and outgoing media. At the end of the outgoing medium for instance, one imposes that the elastic wave is propagating in the forward direction, that is to say is leaving the medium without reflection. The condition is therefore,

$$c_l\partial\vec{u}/\partial y+\partial\vec{u}/\partial t=0, \tag{10}$$

where the longitudinal speed of sound is used for both the x and y components of the displacement field. A finite-difference approximation of that condition, correct to the square of the y and t increment steps, is used.

III. AIR-FILLED TUBES IN WATER

The calculations discussed in this section were carried out for a square lattice of cylindrical polymer tubes in water, with air inside the tubes. The geometry is illustrated in Fig. 1, the lattice parameter is 20 mm. In the absence of polymer coating ($\delta=0$), air cylinders in water give rise to a band structure with little dispersion when placed on a square or hexagonal lattice and when the air filling fraction is between 0.1 and 0.55 [13]. When, as a first approximation, the density ratio between water and air is taken as infinity, the eigenfre-

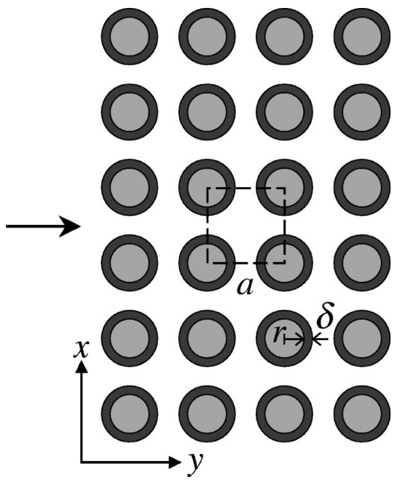

FIG. 1. Two-dimensional cross section of a square array of polymer tubes, with thickness δ and internal radius r. Air occupies the interior of the tubes and there is water at the exterior. The system has an infinite extension in the x direction and is excited by an incident wave packet arriving as indicated by the arrow.

quencies ω of the air cylinders can be obtained from the zeroes of the derivative of the Bessel function of the first kind, $J'_m(\omega r/c)=0$, where c is the speed of sound in air and r is the cylinder radius. This remains approximately true when the finite density of water is taken into account, because for intermediate filling fractions, the propagation of the acoustic waves is predominant in air and the air cylinders only weakly influence each other. The frequencies obtained by band-structure calculations of the first five bands for an infinite periodic system are listed in Table I for a filling fraction close to 0.2. All the bands but the first one have a dispersion smaller than 30 Hz. As indicated by the table, there is a huge band gap in the audible region, between 0.6 and 20 kHz.

The transmission coefficient of the film shown in Fig. 1 was computed as explained above. The reference frequency used for generating the incident wave packet [see Eq. (9)] was $\omega_0/2\pi=20$ kHz. In order to avoid reflections at the interfaces between the film and the external media, 70 mm of the same material (water) as the host containing the air cylinders was used as propagating media on both sides of the film.

The first band of the air-water composite crystal is characterized by a small sound velocity, approximately 30 m/s. In order not to affect this band too much, we chose for the tubes that separate the air from water a polymer having small speeds of sound, of the order of 30 m/s. A butyl rubber (Poly isobutene-co-isoprene) was selected on that ground, the elastic data [16] are given in Table II. Different values of the

TABLE I. Eigenfrequencies of a perfect square lattice of air cylinders in water with radius $r=5$ mm and period $a=20$ mm. m is the order of the Bessel function from which the bands derive.

Band	1 ($m=0$)	2 ($m=1$)	3 ($m=2$)	4 ($m=0$)	5 ($m=3$)
ν (kHz)	0.0–0.6	20.0	33.1	41.6	45.6

TABLE II. Elastic properties of the materials used in the calculations: mass density, longitudinal, and transverse speeds of sound.

	$\rho(\text{kg/m}^3)$	c_l(m/s)	c_t(m/s)
Air	1.3	340	0
Water	1000	1490	0
Polymer	933	55	19

polymer coating thickness were considered, and typical results are shown in Fig. 2 for a film composed of four periods (four rows of cylinders) in the y direction.

For $\delta=0$ (no polymer coating around the air cylinders), there are a few peaks of transmission below 0.6 kHz coming from the first band in Table I. At 1 kHz, the computed transmission has fallen down to 2% (17-db attenuation) and keeps decreasing. The second frequency band of the air-water square lattice gives rise to a small transmission peak at 20 kHz (Fig. 2, top panel). The frequency bands of this composite lattice are so flat that it was difficult to find their signatures in the computed transmission spectrum. A very long time integration (2^{21} time steps of 20 ns) was used for this particular system. When the polymer coating was introduced, 2^{19} time steps were used to investigate the sonic characteristics of the film. The transmission spectrum shown in the top panel of Fig. 2 is fully consistent with that obtained for a cluster of air bubbles in water where the wide gap of transmission is due to multiple-scattering effects [17].

With a polymer tube thickness $\delta=1.25$ mm, there is a

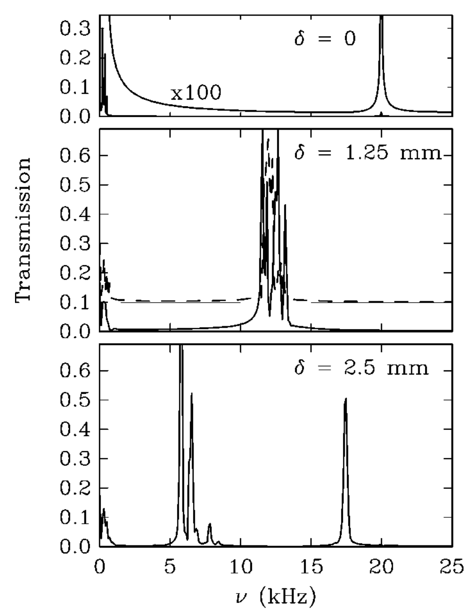

FIG. 2. Solid lines: spectral transmission coefficient of the system shown in Fig. 1 for three values of the thickness of the polymer tubes: $\delta=0$, 1.25, and 2.50 mm. The lattice parameter is 20 mm, four periods are considered in the transverse direction, the inner radius of the tubes (air cylinders) is $r=5$ mm. Dashed line: transmission spectrum of a film composed of 5 rows of tubes ($\delta=1.25$ mm) arranged on the centered square lattice obtained by rotating the unit cell by 45°. This curve has been shifted vertically for clarity.

broad transmission band centered around 12 kHz, and another small peak at 35 kHz (not shown in Fig. 2). The large pass band is obviously due to the polymer, since its frequency changes by increasing the tube thickness. Its position is also dependent on the elastic response of the polymer coating: multiplying its longitudinal velocity c_l by a factor of 2, while keeping c_t constant, shifts the transmission peak to 24 kHz.

Returning to Fig. 2, the transmission level on both sides of the large polymer band is found significantly higher than in the absence of polymer. However, the transmission of the film remains reasonably small, below 2.5%, for ν between 1 and 10 kHz, and above 15 kHz. When $\delta = 2.5$ mm, the frequency of the polymer-induced transmission band decreases by a factor of two (see Fig. 2, bottom panel), and another transmission peak appears at 17.5 kHz. Still, there are two sonic stop bands between 1 and 5 kHz, and between 8.5 and 16.5 kHz, where the computed transmission is found much smaller than the background transmission obtained with $\delta = 1.25$ mm.

By rotating the two-dimensional unit cell by 45° with respect to the incident (y) direction, the properties of the composite crystal can be investigated along the [11] direction in the reciprocal space, instead of [10] as before. As viewed from the incident direction, the cylinders are now arranged on a centered square lattice, with parameter $\sqrt{2}a$. The results for the tube thickness $\delta = 1.25$ mm are shown by the dashed line curve in the central panel of Fig. 2 for a film composed of 5 rows of cylinders (2.5 periods). The transmission spectrum remains essentially the same as with the previous geometry, which indicates that the frequency gaps do not depend on the wave-vector direction.

The number of periods across the film has some influence on the transmission spectrum of the composite medium. This is illustrated in Fig. 3 for a series of films having the original geometry depicted in Fig. 1 and composed of 1 to 5 rows of tubes across thickness. Already with one row of tubes, the essential features of the spectra computed for thicker films are present. A resonance of the air cylinders is clearly visible at 20 kHz but the signature of this mode rapidly disappears by increasing the number of periods. At least two other localized modes are present in the transmission curve of the monolayer film, at 1.0 and 7.2 kHz. These peaks shift upward by increasing the transverse velocity c_t of the polymer. They are much less sensitive to the longitudinal velocity. Like for the air-cylinder resonance, the amplitude of the two polymer-tube resonances rapidly decreases by increasing the number of periods along y. This is because the width of the resonances decreases and eventually becomes smaller than the spectral resolution used in our calculations (100 Hz). A test calculation performed for the four-period film with 25-Hz resolution (the same as for the top panel of Fig. 2) revealed the presence of narrow peaks at 1.05, 7.25, and 19.9 kHz. The main transmission band around 12 kHz remains strong in all cases. Interestingly, the background transmission in the wings of the band, around 5 and 17 kHz, is found smaller with 3 periods than with 2 and 4 periods. With 5 periods, the background transmission is again smaller. The origin of this oscillatory behavior is unknown.

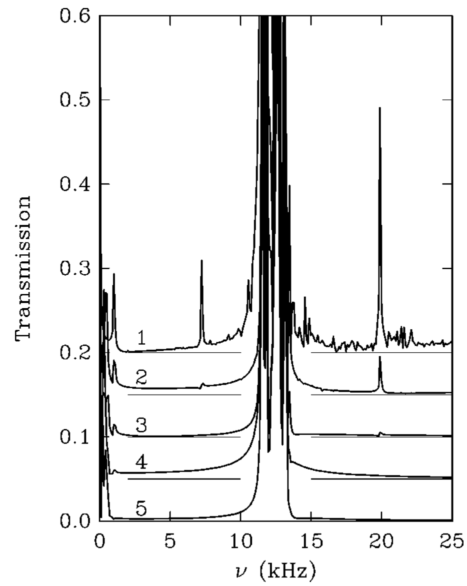

FIG. 3. Spectral transmission coefficient of a square array of polymer tubes in water (inner radius 5 mm, thickness 1.25 mm) composed of 1, 2, 3, 4, and 5 periods in the transverse direction. The curves have been shifted vertically by 0.05 units for clarity.

The use of tubes with very small speeds of sound was essential to preserve part of the sonic band gaps of the original air-water system. With a hard material such as PVC for instance, the transmission of the film shown in Fig. 1 has been found oscillating between 0.8 and 1 for all frequencies between 0 and 25 kHz (no gap in the audible domain).

IV. WATER-FILLED TUBES IN AIR

From a practical point of view, it would be more interesting to have the water contained in tubes with air outside, rather than the opposite. However, water cylinders in air give rise to allowed acoustic bands with much larger dispersion than air cylinders in water [13]. The most favorable situation arises at the close-packing limit since, then, the air cavities between the cylinders become isolated from each other, very much like in the previous section. That close-packing lattices in air are characterized by large acoustic band gaps has been demonstrated for various systems in the all-fluid approximation [8,18,19]. In this respect, one of the best systems is the honeycomb lattice [8,18].

To explore this geometry in transmission, FDTD calculations were performed for a close-packed array of tubes on a honeycomb lattice with hexagonal edge size 11.5 mm (lattice parameter $a = 19.9$ mm). The tubes were supposed to be made of the same polymer as before, with a thickness of 1.25 mm (the inner diameter is 9 mm). There is water inside the tubes and air outside. The transmission coefficient was computed for the two films shown in Fig. 4, which present either a zigzag or an armchair configuration of the tubes at the surface. Air slices 11 mm tick were considered on both sides of the film to generate the incident wave-packet upstream ($\omega_0/2\pi = 45$ kHz) and to record the transmitted signal downstream. Time integration of the equations was performed over 2^{21} steps of 8.3 ns. For the two configurations of

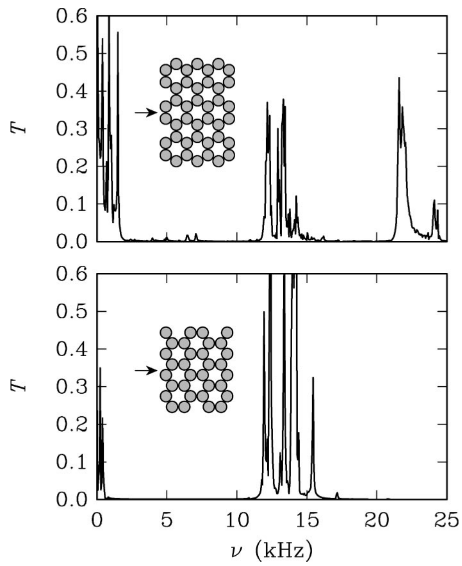

FIG. 4. Spectral transmission coefficient for an array of touching polymer tubes filled with water and located on a honeycomb lattice in air (tube inner radius 4.5 mm, thickness 1.25 mm, hexagonal lattice parameter 19.9 mm). Two configurations of the film are shown, corresponding to an incident wave packet (arrow) propagating along the ΓX (bottom) and ΓJ (top) symmetry lines of the first Brillouin zone. The overall thickness of the film is 71 mm (top) and 69 mm (bottom).

the honeycomb structure, Fig. 4 shows that there is a strong attenuation band between 2 and 11 kHz, and there is another transmission gap between 17.5 and 21 kHz. By comparison, band-structure calculations performed for the honeycomb lattice of touching cylinders of water in air (no envelope) [18] lead to a first absolute band gap extending from 2.6 kHz ($0.15c/a$, with c the speed of sound in air) to 13.9 kHz ($0.82c/a$). Interestingly, with the zigzag arrangement of the tubes (bottom of Fig. 4), the band gap settles at a much lower frequency, around 0.8 kHz, in close analogy with the air-filled tubes in water depicted in the central part of Fig. 2. The pass band between 12 and 14 kHz (central panel of Fig. 2) also comes out in the present geometry and finds its origin in the polymer coating but also in the water cylinders. With the armchair geometry illustrated in the top panel of Fig. 4, there are a two small peaks in the first gap, near 6.8 kHz. These peaks may have the same origin as the one observed at 7.2 kHz in Fig. 3 for small film thickness.

V. CONCLUSIONS

Two-dimensional fluid-fluid composites have interesting phononic properties for they may give rise to large intervals of forbidden acoustic frequencies. Any practical applications of these systems as sonic insulators for instance would require two amendments. First, solid envelopes are necessary to separate the two fluids and, second, the composite medium must be of finite thickness. These are two difficult requirements to explore theoretically, because mixing fluids and solids causes serious convergence problem in plane-wave expansions usually used in band-structure calculations and, furthermore, the finite thickness destroys the periodicity in one direction.

This paper aimed at exploring the effects of these two requirements. The transmission coefficient across a film made of a two-dimensional composite medium was calculated numerically with the FDTD methodology applicable to solid-fluid composites. It was shown that air cylinders in water may lead to a large attenuation band starting at 1 kHz, typically, and extending over about 10 kHz, provided the air be contained in elastically-soft tubes. These results were obtained with tubes on a square lattice with a parameter (20 mm) much smaller than the stopped wavelengths. The upper limit of the sonic gap depends on the thickness of the tube and on its longitudinal speed of sound. The lower limit depends on the air-filling fraction and on the transverse velocity of the tube material. A few, narrow-resonance transmission peaks may exist inside the gap. In our calculations, there was one such resonance at 7.2 kHz.

Another system, with water now contained in a close-packed array of polymer tubes on a honeycomb lattice in air also shows an attenuation band starting slightly below 1 kHz and ending at 11 kHz, with again a lattice parameter a of about 20 mm. In both cases, the use of an elastically-soft polymer to separate the air from water made it possible to maintain the lower limit of the first band gap around $0.06c/a$, typical of the periodic arrays of air cylinders in water. The sonic crystals studied in this paper have the property of exhibiting large acoustic band gaps in the audible frequency range while the thickness of the sample remains small, of the order of a few cm. Furthermore, these sonic crystals are essentially made of water and air, which cost nothing.

ACKNOWLEDGMENTS

P.L. gratefully acknowledges the hospitality of the UFR de Physique of the University of Lille I. The authors acknowledge Le Center de Ressources Informatiques (CRI) and Le Fond Européen de Développement Regional for providing some of the computer facilities. This work was made possible partly thanks to the Convention 991/4269 FIRST-Europe (''Objectif 1'') from the Walloonia Region of Belgium and the European Union. Helpful discussions with Cécile Goffaux are also greatly acknowledged.

[1] Z. Liu, X. Zhang, Y. Mao, Y.Y. Zhu, Z. Yang, C.T. Chan, and P. Sheng, Science **289**, 1734 (2000).
[2] E. Yablonovitch, Phys. Rev. Lett. **58**, 2059 (1987).
[3] M.S. Kushwaha, P. Halevi, L. Dobrzynski, and B. Djafari-Rouhani, Phys. Rev. Lett. **71**, 2022 (1993).
[4] M.M. Sigalas, and E.N. Economou, Solid State Commun. **86**, 141 (1993).
[5] F.R. Montero de Espinosa, E. Jiménez, and M. Torres, Phys. Rev. Lett. **80**, 1208 (1998).
[6] J.V. Sánchez-Pérez, D. Caballero, R. Mártinez-Sala, C. Rubio,

J. Sánchez-Dehesa, F. Meseguer, J. Llinares, and F. Gálvez, Phys. Rev. Lett. **80**, 5325 (1998).
[7] J.O. Vasseur, P.A. Deymier, G. Frantziskonis, G. Hong, B. Djafari-Rouhani, and L. Dobrzynski, J. Phys.: Condens. Matter **10**, 6051 (1998).
[8] D. Caballero, J. Sánchez-Dehesa, C. Rubio, R. Mártinez-Sala, J.V. Sánchez-Pérez, F. Meseguer, and J. Llinares, Phys. Rev. E **60**, R6316 (1999).
[9] D. García-Pablos, M. Sigalas, F.R. Montero de Espinosa, M. Torres, M. Kafesaki, and N. García, Phys. Rev. Lett. **84**, 4349 (2000).
[10] M.M. Sigalas and N. Garcia, Appl. Phys. Lett. **76**, 2307 (2000).
[11] M.M. Sigalas and N. García, J. Appl. Phys. **87**, 3122 (2000).
[12] Y. Tanaka, Y. Tomoyasu, and S. Tamura, Phys. Rev. B **62**, 7387 (2000).
[13] M.S. Kushwaha and B. Djafari-Rouhani, J. Appl. Phys. **84**, 4677 (1998).
[14] *Advances in Computational Electrodynamics*, edited by A. Taflove (Artech House, London, 1999), p. 91.
[15] G. Mur, IEEE Trans. Electromagn. Compat. **23**, 377 (1981).
[16] Polymer Handbook, 3rd Ed., edited by J. Braudrup and E. H. Immergut (Wiley, Wiley-Interscience, New York, 1989).
[17] M. Kafesaki, R.S. Penciu, and E.N. Economou, Phys. Rev. Lett. **84**, 6050 (2000).
[18] J.O. Vasseur, B. Djafari-Rouhani, L. Dobrzynski, and P.A. Deymier, J. Phys.: Condens. Matter **9**, 7327 (1997).
[19] M.S. Kushwaha, Appl. Phys. Lett. **70**, 3218 (1997).